NASA Technical Paper 2140

March 1983

Sliding Induced Crystallization of Metallic Glass

Kazuhisa Miyoshi
and Donald H. Buckley

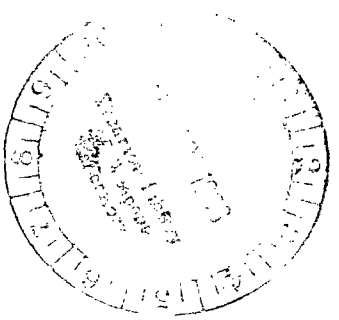

NASA

NASA
Technical
Paper
2140

1983

Sliding Induced Crystallization of Metallic Glass

Kazuhisa Miyoshi
and Donald H. Buckley
Lewis Research Center
Cleveland, Ohio

National Aeronautics
and Space Administration

**Scientific and Technical
Information Branch**

Trade names or manufacturers' names are used in this report for identification only. This usage does not constitute an official endorsement, either expressed or implied, by the National Aeronautics and Space Administration.

SUMMARY

Sliding friction and wear experiments, electron microscopy, and diffraction studies were conducted to examine the metallurgical microstructure of a metallic glass surface strained in sliding friction and wear. Friction and wear experiments were conducted with 6.4- and 3.2-millimeter-diameter aluminum oxide spheres sliding, in reciprocating motion, on a metallic glass with a composition of $Fe_{67}Co_{18}B_{14}Si_1$ at a sliding velocity of 1.5 millimeters per second, with a load of 2.5 newtons, at room temperature, and in a laboratory air atmosphere.

The results of the investigation indicate that the amorphous alloy (metallic glass) can be crystallized during the sliding process. Crystallites with a size range of 10 to 150 nanometers are produced on the wear surface of the amorphous alloy. Crystallization of the wear surface of the amorphous alloy causes an increase in friction. Plastic flow occurred on the amorphous alloy with sliding, and the flow film of the alloy transferred to the aluminum oxide surface. Two distinct types of wear debris were observed as a result of sliding: an alloy wear debris, and powdery and whiskery wear debris particles. Generating oxide wear debris particles on the amorphous alloy causes transitions in friction behavior. Oxide wear debris particles can contribute to increased friction of the alloy when in the amorphous state. In contrast, however, they can contribute to a decrease in the friction of the wear surface of the alloy when in the crystalline state.

INTRODUCTION

Metallic glasses are currently finding increased application in the aerospace industry (ref. 1). They are used for joining internal assemblies in gas turbines. Nickel-based brazed foils of the BNi class are replacing the more expensive gold-based BAu-4 foils in engine valves and many other components. However, like BAu-4, the nickel-based filler metals have excellent flow behavior, are compatible with most stainless steels and nickel alloys, and offer an outstanding combination of high-temperature strength, fatigue properties, and oxidation and corrosion resistance (ref. 1).

A combination of favorable mechanical and physical properties makes metallic glasses candidates for other technological applications. For example, the combination of high permeability and high hardness makes these materials suitable for use in highly developed magnetic recording devices (e.g., video tape recorders). In most high-density devices, a magnetic head in sliding contact with a magnetic tape is used for recording and playback. Therefore, the magnetic head and tape must have good wear resistance. Metallic glasses can also be used in foil bearings. The highly disordered structures of metallic glass would be resistant to radiation damage, and, thus, have potential for use where constant mechanical properties are required under irradiation. The mechanical and physical properties of metallic glasses are, therefore, of basic scientific interest.

Metallic glasses have several properties that make them attractive for tribological applications. These properties include great adhesion, shear strength, impact penetration, corrosion resistance, stiffness, and ductility. Relatively little research, however, has been done on the tribological properties of the metallic glasses (refs. 2 to 4).

The coefficients of friction have been determined for some metallic glasses ($Ni_{40}Fe_{40}P_{14}B_6$, $Ni_{36}Fe_{32}Cr_{14}P_{12}B_6$, $Ni_{49}Fe_{29}P_{14}B_6Si_2$, $Fe_{80}B_{20}$, and $Fe_{80}P_{16}C_3B_1$) in sliding contact with a small ball bearing sphere (ref. 2). Unfortunately, the experimental conditions, such as temperature, environment, sliding speed, and ball diameter are not described in the reference. Temperature significantly influences the friction properties as well as the elemental composition on the surface and the microstructure of metallic glasses (refs. 3 and 4). The corresponding alloys generally exhibit higher coefficients of friction in the crystalline state than they do in the glassy (amorphous) state.

Metallic glasses consist largely of random aggregates of atoms, their densities being only slightly different from the densities of crystals having the same compositions (ref. 5). Also, although metallic glasses are elastically stiffer than silicate glasses, they are not brittle and have considerable ability to deform plastically. In the sliding, rolling, or rubbing contact of materials, the surfaces become strained as a result of the mechanical activity that takes place.

On a crystalline surface, however, the crystallinity and crystallographic orientation can be changed markedly by the strain. The higher the degree of strain, the lower the temperature for recrystallization. Consequently, a highly strained crystalline surface tends to promote recrystallization of the solid surface long before the surface may otherwise be ready for such recrystallization.

The tribological surface can also contain grains which are highly oriented as a result of the sliding, rolling, or rubbing process. In other words, the grains tend to become reoriented at the surface so as to reflect the effects of the mechanical parameters imposed on the surface. Such reorientation and recrystallization of crystalline solids in the sliding, rolling, or rubbing process are well known (refs. 6 to 8). However, we do not know what actually happens on the tribological surface of metallic glasses during sliding friction and wear. Does, for example, the amorphous state of the metallic glass surface crystallize and become crystallographically oriented in the tribological process?

This investigation examines the metallurgical microstructure of a metallic glass surface strained in friction and wear experiments. These experiments were conducted with 6.4- and 3.2-millimeter-diameter aluminum oxide spheres sliding, in reciprocating motion, on the $Fe_{67}Co_{18}B_{14}Si_1$ metallic glass at a sliding velocity of 1.5 millimeters per second, with a load of 2.5 newtons (250 g), at room temperature, and in a laboratory air atmosphere.

MATERIALS

The composition of the metallic glass investigated herein and some of its properties are listed in table I. The alloy was in the form of a ribbon (0.030- to 0.033-mm-thick foil) and was used in the as-cast condition. The spherical riders that were made to slide on the foil were single-crystal aluminum oxide (sapphire), and the diameters of the spheres were 3.2 and 6.4 millimeters (1/8 and 1/4 in.). The microhardness (Vickers) of the metallic glass was 980 at an indentation load of 1 newton.

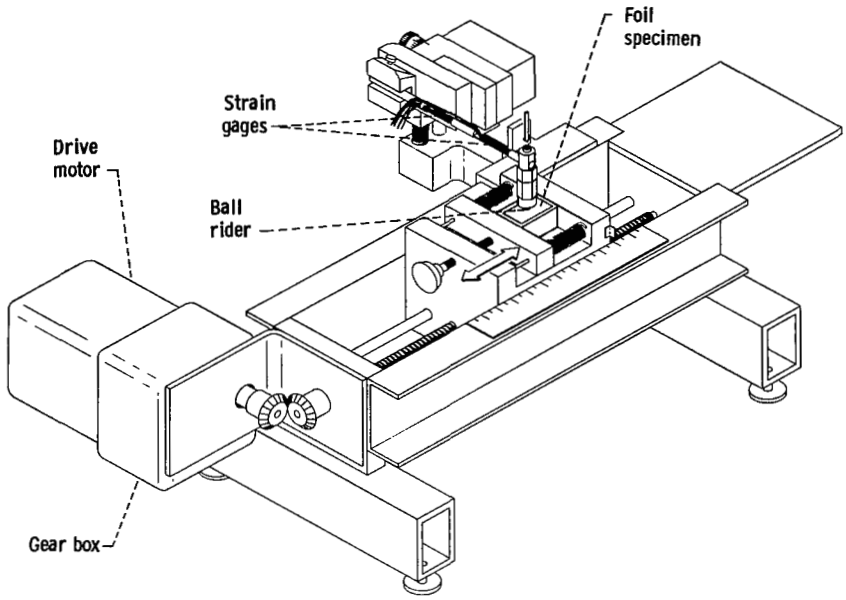

Figure 1. - Friction and wear apparatus.

TABLE I. - PROPERTIES OF A METALLIC GLASS

Alloy composition[a]	$Fe_{67}Co_{18}B_{14}Si_1$
Vickers microhardness	980
Crystallization temperature[a], °C	430
Density[a], g/cm^3	7.56
Ultimate tensile strength[a], GPa	1.5
Bend ductility[a,b]	1
Thickness, μm	30 to 33

[a]Manufacturer's analysis.

[b]$\varepsilon = t/(d-t)$: t, ribbon thickness; d, micrometer spacing at bend fracture.

APPARATUS

The apparatus used in this investigation (fig. 1) was basically a pin (rider) on a flat configuration. The specimen was mounted on hardened steel flats and retained in a vise mounted on a screw-driven platform. The platform was driven reciprocally back and forth by a mechanical drive system containing a gear box, a set of bevel gears, and a lead screw driven by an electric motor. The rider traversed a distance of 10 millimeters on the surface of the foil. Microswitches at each end of the traverse reversed the direction of travel so that the rider retraced the original track from the opposite direction; this process was repeated continuously. The rider was deadweight loaded against the foil. The arm retaining the rider contained the strain gages to measure the tangential force. The entire apparatus was housed in a plastic box.

EXPERIMENTAL PROCEDURE

The metallic glass foil and the rider specimen surfaces were scrubbed with levigated alumina, rinsed with tap water and then distilled water, and finally rinsed with ethyl alcohol. After the surfaces were dried with nitrogen gas, the specimens were placed in the experimental apparatus. The specimen surfaces were then brought into contact and loaded, and the friction and wear experiments began. Three sets of experiments were conducted, and each one was continued for 3 or 150 hours.

To determine the causes of transitions in friction behavior of metallic glass, two sets of experiments were conducted. In the first set, the friction and wear experiments were run for 3 hours and then the rider specimen was replaced with a new rider specimen and the foil surface was cleaned with ethyl alcohol. The experiments were then continued for an additional 3 hours. The rider specimen was again replaced with a new rider and the foil surface was again cleaned with ethyl alcohol. The experiments were run for a final period of 3 hours.

In the second set, the friction and wear measurements were continued for 150 hours, and then the rider specimen was replaced with a new rider and the foil surface was cleaned with ethyl alcohol. The experiments were then continued in the same manner as the first set. In both sets of experiments, the new riders traveled and retraced the original track.

RESULTS AND DISCUSSION

Friction and Wear Behavior

Friction and wear experiments were conducted with $Fe_{67}Co_{18}B_{14}Si_1$ amorphous alloy and 304 stainless steel in contact with 6.4- and 3.2-millimeter-diameter aluminum oxide spherical riders. When the amorphous alloy and the 304 stainless steel were rubbed by the 6.4-millimeter aluminum oxide rider at a load of 2.5 newtons for 30 minutes, there was very little difference in friction behavior between the two alloys. The coefficients of friction for the amorphous alloy and 304 stainless steel were 0.2 and 0.18, respectively. The wear results were markedly different when examined by optical and scanning electron microscopies. Essentially no detectable wear existed on the surface of the amorphous alloy. However, considerable wear was indicated on the 304 stainless steel, as shown in the scanning electron micrograph of figure 2.

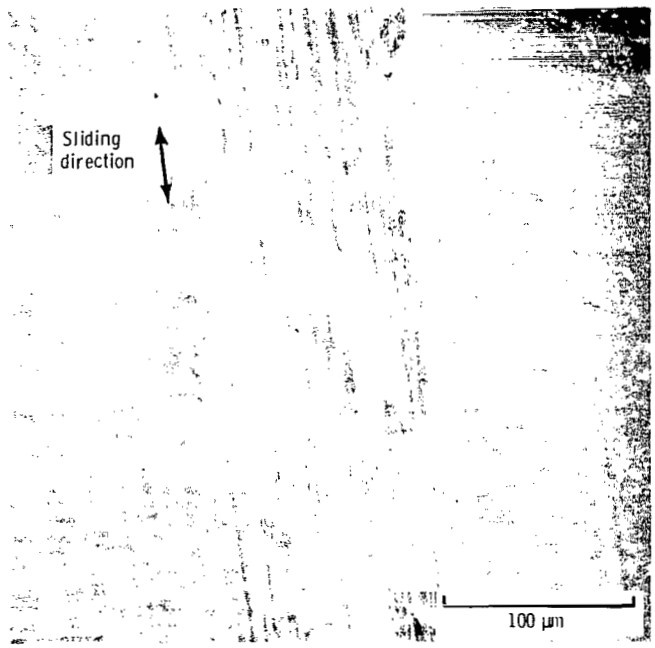

Figure 2. - Photomicrograph of 304 stainless steel wear surface. Rider, 6.4-millimeter-diameter aluminum oxide sphere; load, 2.5 newtons; sliding velocity, 1.5 millimeters per second; dry sliding in laboratory air atmosphere.

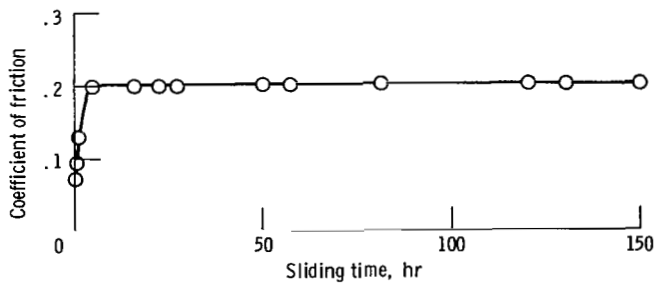

Figure 3. - Coefficient of friction as function of sliding time for $Fe_{67}Co_{18}B_{14}Si_1$ amorphous alloy in laboratory air atmosphere. Rider, 3.2-millimeter-diameter aluminum oxide sphere; load, 2.5 newtons; sliding velocity, 1.5 millimeters per second; room temperature.

Considerable plastic flow occurred, and a copious amount of oxide debris was generated on the 304 stainless steel. Lumps of metal appeared in the wear track.

Since no visible wear was observed on the amorphous alloy, sliding friction experiments were conducted with a smaller sphere (0.32-mm-diam aluminum oxide rider) at a sliding time extended to 150 hours to provide a high contact pressure and a more severe experiment.

Although friction was initially low, it increased with increasing sliding time as indicated in figure 3. After some time, an equilibrium condition was reached, and the friction did not change with sliding time. The coefficients of friction shown in figure 3 are generally the same as those obtained at the lower loads of 0.2 to 1.0 newton. The results obtained from experiments conducted with 0.64-millimeter-diameter aluminum oxide rider at loads of 0.1 to 2.5 newtons are also consistent with those shown in figure 3.

Scanning electron micrographs of a typical wear track on the amorphous alloy and a wear scar on the aluminum oxide surface are shown in figure 4. The experiment was conducted at a load of 2.5 newtons with a 0.32-millimeter-diameter aluminum oxide rider for a total sliding time of 5 hours. Oxide wear debris particles were generated on the amorphous alloy surface. The aluminum oxide rider surface contacted by the amorphous alloy had alloy as well as oxide wear debris particles transferred to it. However, an examination of the wear tracks indicated an undetectable difference in the surface profiles measured before and after the experiment. Therefore, it was concluded that the amount of wear was negligible.

Figure 5 illustrates a detailed examination of the oxide wear debris (submicrometer to micrometers in size) produced on the amorphous alloy by sliding the 3.2-millimeter-diameter aluminum oxide rider on the alloy for 5 hours. The scanning electron micrographs clearly reveal powdery and whiskery oxide wear debris particles on and near the wear track.

Figures 6 and 7 present scanning electron micrographs of typical wear tracks and scars in which oxide wear debris particles were removed from the surface. The wear tracks and scars were produced during a 5-hour sliding period. After the sliding friction experiment, the amorphous alloy specimen and aluminum oxide rider were cleaned with ethyl alcohol and dried. Figures 6 and 7 illustrate that plastic flow occurs on the amorphous alloy with repeated sliding and that the flow film of the alloy adheres and transfers to the aluminum oxide rider.

During a 150-hour sliding period, considerable plastic flow occurred and considerable oxide debris was generated on the amorphous alloy. Figure 8(a) reveals evidence of wear damage and large particles of wear debris, which were generated at local spots. Shear fracture occurs at very local areas in the amorphous alloy during repeated sliding. Figure 8(b) presents wear debris of the amorphous alloy.

The surface profile of the wear track on the amorphous alloy presented in figure 9 reveals a considerable amount of wear. The wear volume was 0.01 cubic millimeter or less. The wear rate, which is defined as the quantity of amorphous alloy removed under a unit load and with a unit distance of sliding, was 5×10^{-9} cubic millimeter per newton-millimeter or less.

Figures 10 and 11 present scanning electron micrographs of a wear scar on the aluminum oxide rider for a sliding period of 150 hours. Figure 10 indicates that the amorphous alloy transfer to the rider is much more than that obtained when the sliding period is only 5 hours (fig. 4(b)). Figure 10 also reveals that the sliding produced a multilayer film structure of the amorphous alloy transfer. This film structure is produced by the piling up of the amorphous alloy wear debris.

Figure 11 reveals oxide as well as amorphous alloy wear debris (submicrometers to micrometers in size) transferred to the aluminum oxide rider. The scanning micrographs in figure 11 clearly reveal powdery and whiskery wear debris particles.

Metallurgical Structure

The microstructure was examined by transmission electron microscopy and diffraction in a microscope operating at 100 kilovolts to establish the exact crystalline state of the amorphous alloy foils. Final thinning of the foils was accomplished by electropolishing.

A typical example of the structure of the as-received amorphous alloy is shown in figure 12, in which no dislocations or grain boundaries are evident.

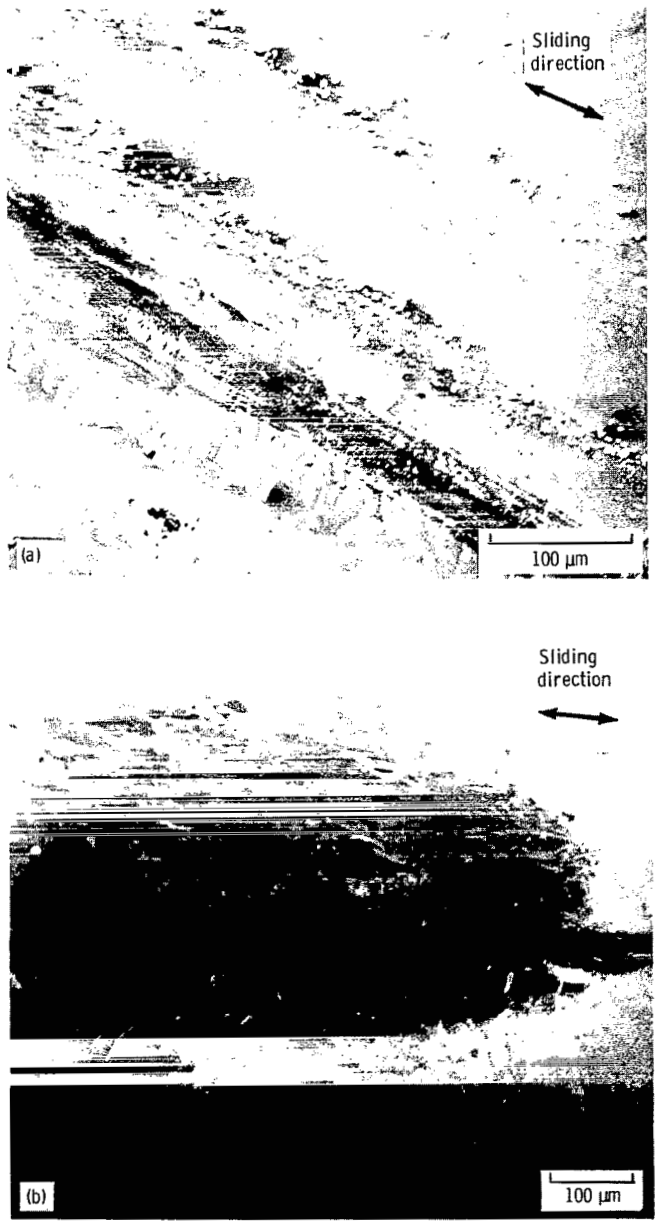

(a) Wear track on $Fe_{67}Co_{18}B_{14}Si_1$ amorphous alloy.

(b) Wear scar on aluminum oxide rider.

Figure 4. - Scanning electron micrographs of wear track on $Fe_{67}Co_{18}B_{14}Si_1$ amorphous alloy and wear scar on aluminum oxide rider. Rider, 3.2-millimeter-diameter aluminum oxide sphere; load, 2.5 newtons; sliding velocity, 1.5 millimeters per second; sliding time, 5 hours; sliding distance, 27 meters; room temperature; laboratory air atmosphere.

(a) Powdery wear debris particles.

(b) Whiskery wear debris particles.

Figure 5. - Scanning electron micrographs of powdery and whiskery wear debris particles produced on $Fe_{67}Co_{18}B_{14}Si_1$ amorphous alloy. Rider, 3.2-millimeter-diameter aluminum oxide sphere; load, 2.5 newtons; sliding velocity, 1.5 millimeters per second; sliding time, 5 hours; sliding distance, 27 meters; room temperature; laboratory air atmosphere.

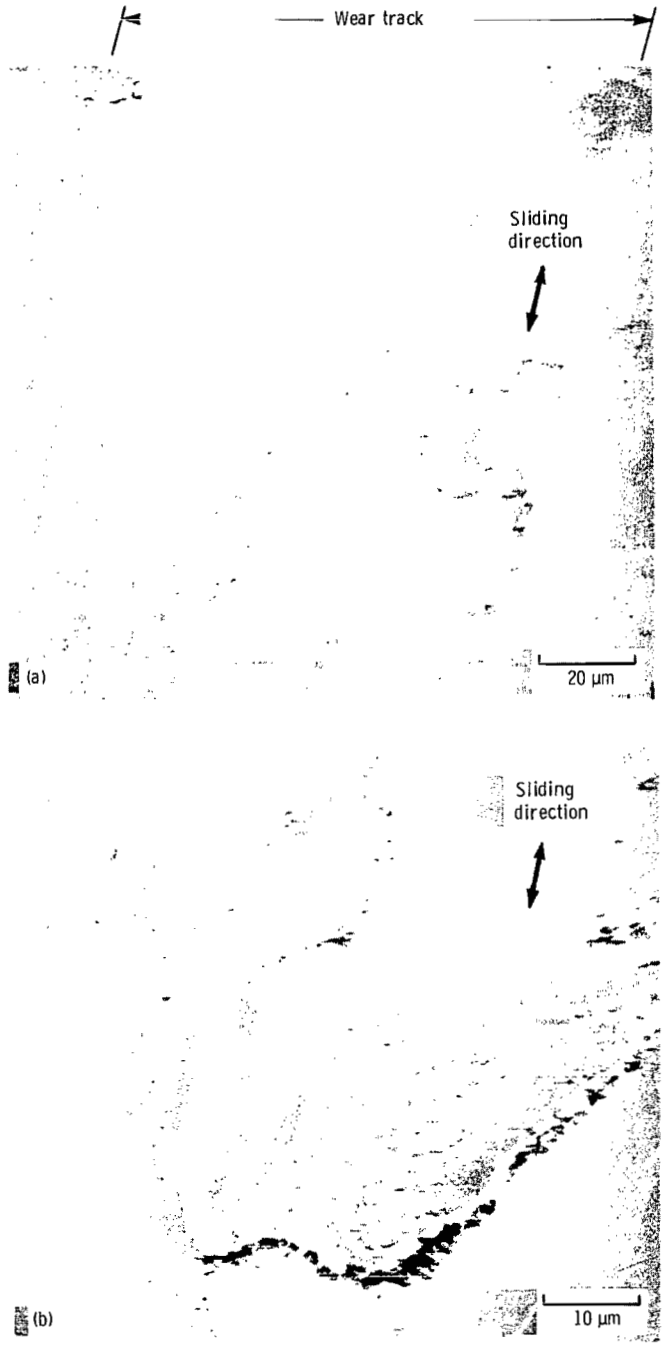

(a) Low magnification.

(b) High magnification.

Figure 6. - Scanning electron micrographs of wear track on $Fe_{67}Co_{18}B_{14}Si_1$ amorphous alloy. Rider, 3.2-millimeter-diameter aluminum oxide sphere; load, 2.5 newtons; sliding velocity, 1.5 millimeters per second; sliding time, 5 hours; sliding distance, 2.7 meters; room temperature; laboratory air atmosphere.

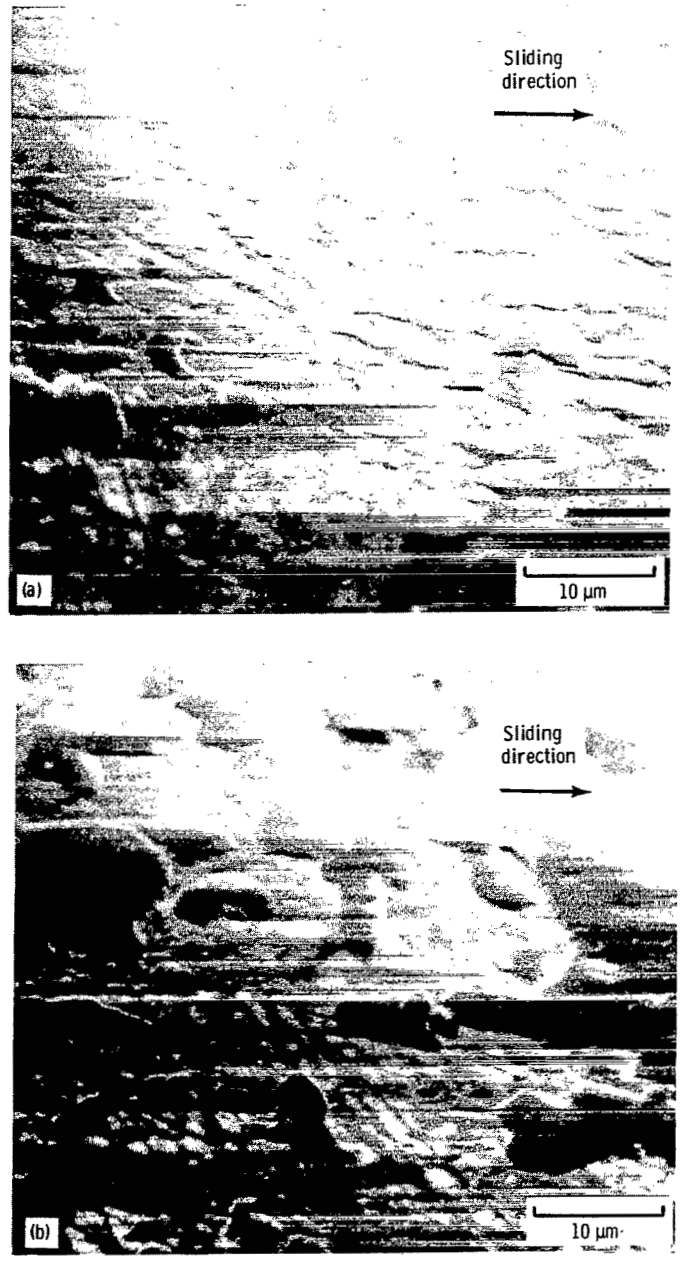

(a) Uniform transfer.

(b) Nonuniform transfer.

Figure 7. - Scanning electron micrographs of near scar on aluminum oxide rider sliding on $Fe_{67}Co_{18}B_{14}Si_1$ amorphous alloy surface. Rider, 3.2-millimeter-diameter aluminum oxide sphere; load, 2.5 newtons; sliding velocity, 1.5 millimeters per second; sliding time, 5 hours; sliding distance, 2.7 meters; room temperature; laboratory air atmosphere.

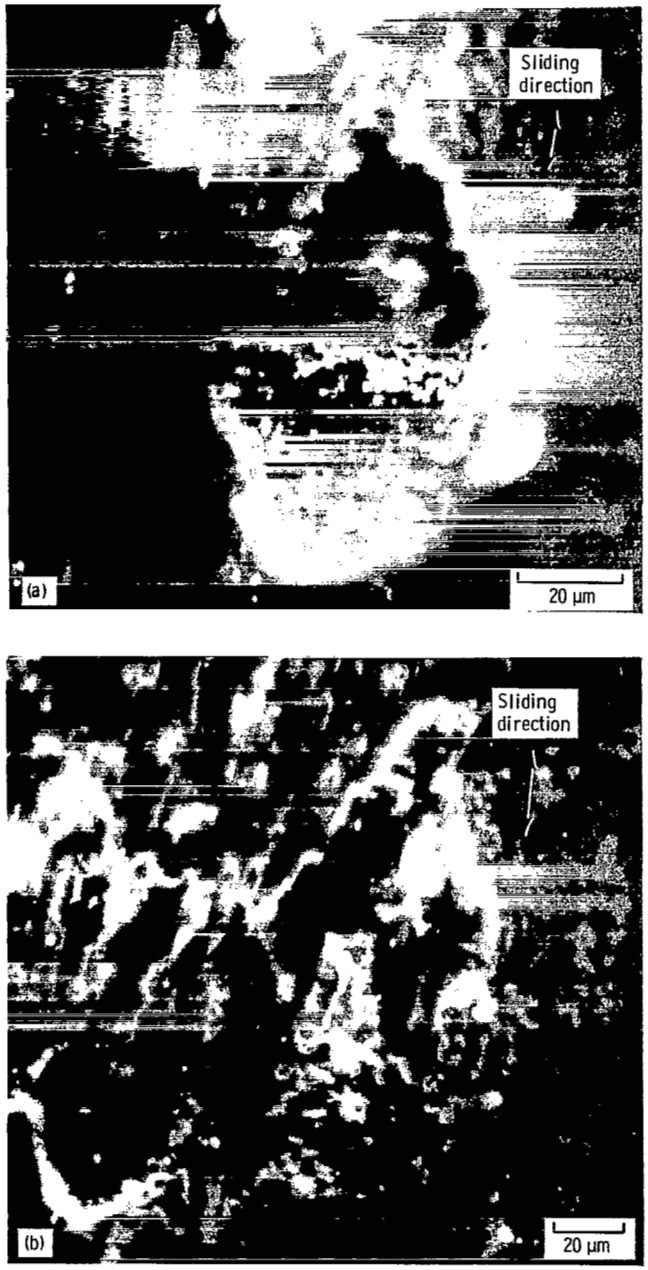

(a) Wear damage.

(b) Back-transferred wear debris.

Figure 8. - Scanning electron micrographs of wear track on $Fe_{67}Co_{18}B_{14}Si_1$ amorphous alloy at sliding period of 150 hours. Rider, 3.2-millimeter-diameter aluminum oxide sphere; load, 2.5 newtons; sliding velocity, 1.5 millimeters per second; sliding time, 150 hours; sliding distance, 810 meters; room temperature; laboratory air atmosphere.

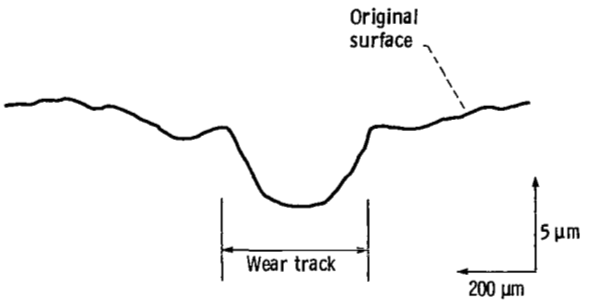

Figure 9. - Surface profile across wear track generated by aluminum oxide rider sliding on $Fe_{67}Co_{18}B_{14}Si_1$ amorphous alloy in laboratory air atmosphere. Rider 3.2-millimeter-diameter aluminum oxide sphere; load, 2.5 newtons; sliding velocity, 1.5 millimeters per second; sliding time, 150 hr; sliding distance 810 meters; room temperature.

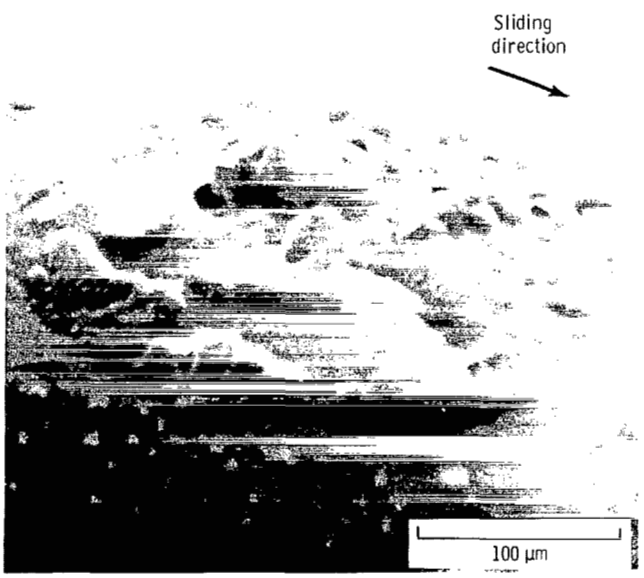

Figure 10. - Scanning electron micrograph of wear scar on aluminum oxide rider sliding on $Fe_{67}Co_{18}B_{14}Si_1$ amorphous alloy in laboratory air atmosphere. Rider, 3.2-millimeter-diameter aluminum oxide sphere; load, 2.5 newtons; sliding velocity, 1.5 millimeters per second; sliding time, 150 hours; sliding distance, 810 meters; room temperature.

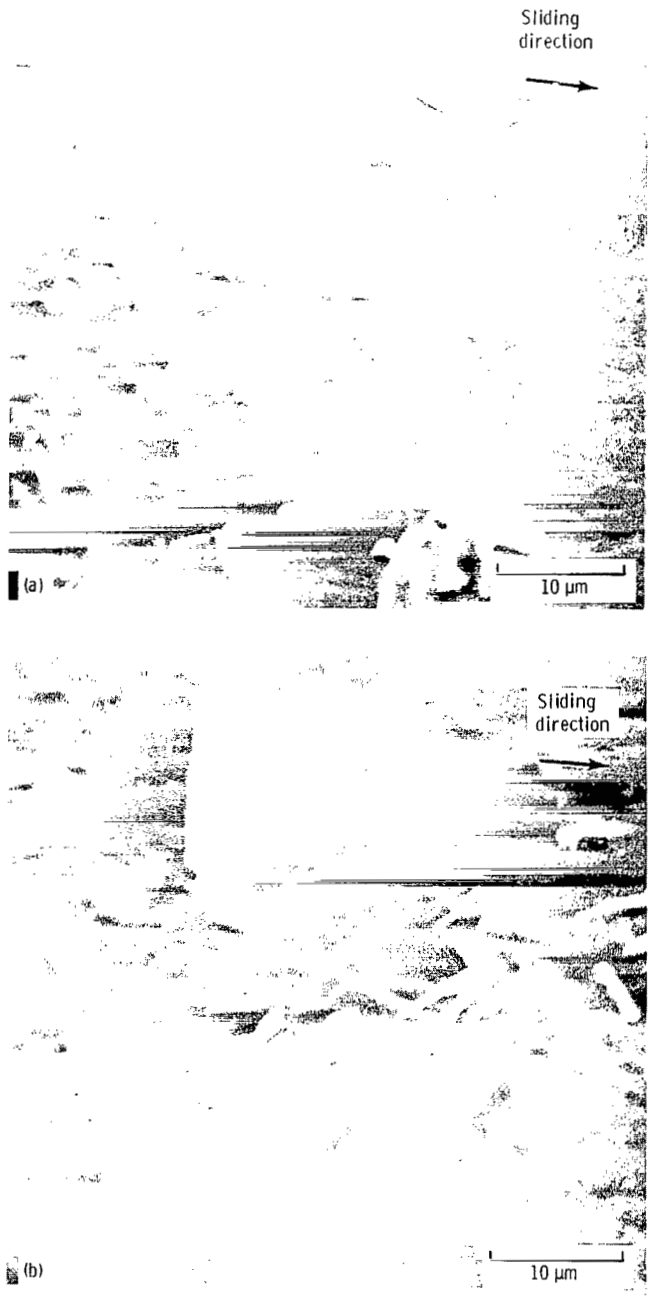

(a) Powdery wear debris particles.

(b) Whiskery wear debris particles.

Figure 11. - Scanning electron micrographs of powdery and whiskery wear debris particles produced on $Fe_{67}Co_{18}B_{14}Si_1$ amorphous alloy and then transferred to aluminum oxide rider during sliding. Rider, 3.2-millimeter-diameter aluminum oxide sphere; load, 2.5 newtons; sliding velocity, 1.5 millimeters per second; sliding time, 150 hours; sliding distance, 810 meters; room temperature; laboratory air atmosphere.

However, black spots, believed to be crystallites ranging in size from 1.5 to 4.0 nanometers, are apparent in the micrograph. The transmission electron diffraction patterns for the as-received foil are also presented in figure 12. The pattern indicates that the amorphous alloy was not completely amorphous, but contained extremely small grains of approximately a few nanometers in size.

A typical example of the wear surface of the amorphous alloy run for 150 hours is shown in figure 13. Dark dots, which are believed to be crystallites ranging in size from 10 to 50 nanometers, are apparent. The electron diffraction pattern indicates that the wear surface contained small crystalline grains.

Figure 14 presents bright and dark field images and the diffraction pattern of a local area of the wear surface on the amorphous alloy. Dark spots observed in the bright image are reversed in the dark image; the diffraction pattern was taken from the spots. Figure 14 clearly indicates crystallization due to mechanical processing (sliding friction) on the amorphous alloy surface. The diffraction pattern is essentially that of a crystalline nature. Thus, crystallites with sizes of 10 to 150 nanometers are produced on the wear surface of the amorphous alloy during sliding.

Transitional Friction and Wear Behavior

As mentioned previously, oxide and amorphous alloy wear debris are produced during the wear process. The generation of powdery and whiskery wear debris may cause a change in friction and wear during sliding. This phenomenon is exemplified in the data of figure 15(a).

Figure 15(a) presents the coefficient of friction as a function of sliding time. The aluminum oxide rider and the amorphous alloy foil were cleaned with ethyl alcohol and dried before they were brought into contact. The coefficient of friction increased with increasing sliding time to 3 hours, when the sliding friction experiment was stopped. The aluminum oxide rider was replaced with a clean aluminum oxide rider. Oxide wear debris particles produced in the first 3 hours of sliding were removed from the wear track of the amorphous alloy with ethyl alcohol and the wear track was dried.

The friction experiment was then restarted with the new aluminum oxide rider sliding directly on the wear track of the amorphous alloy. At the beginning of this second sliding friction experiment, the coefficient of friction was low and was almost the same as that of the first sliding friction experiment. The coefficient of friction increased with increasing sliding time, and after a sliding period of 6 hours it was the same as that obtained after 3 hours.

A third sliding friction experiment was conducted in the same manner as the second one. At the beginning of this experiment, the coefficient of friction was low and was almost the same as that of the first and second experiments. At the end of each sliding friction experiment, oxide wear debris particles were observed (see figs. 4 and 5). Thus, the transient friction shown in figures 3 and 15(a) is primarily due to the generation of oxide wear debris particles.

Figure 15(b) also presents the coefficient of friction as a function of sliding time. After a sliding period of 150 hours, the wear surface of the amorphous alloy was cleaned with ethyl alcohol and then dried. The aluminum oxide rider was replaced with a new rider. This rider was slid directly on the wear track of the amorphous alloy. Figure 15(b) shows that the coefficient of friction at the beginning of the second experiment (after 150 hr of sliding) was higher than that of the first experiment. The high coefficient

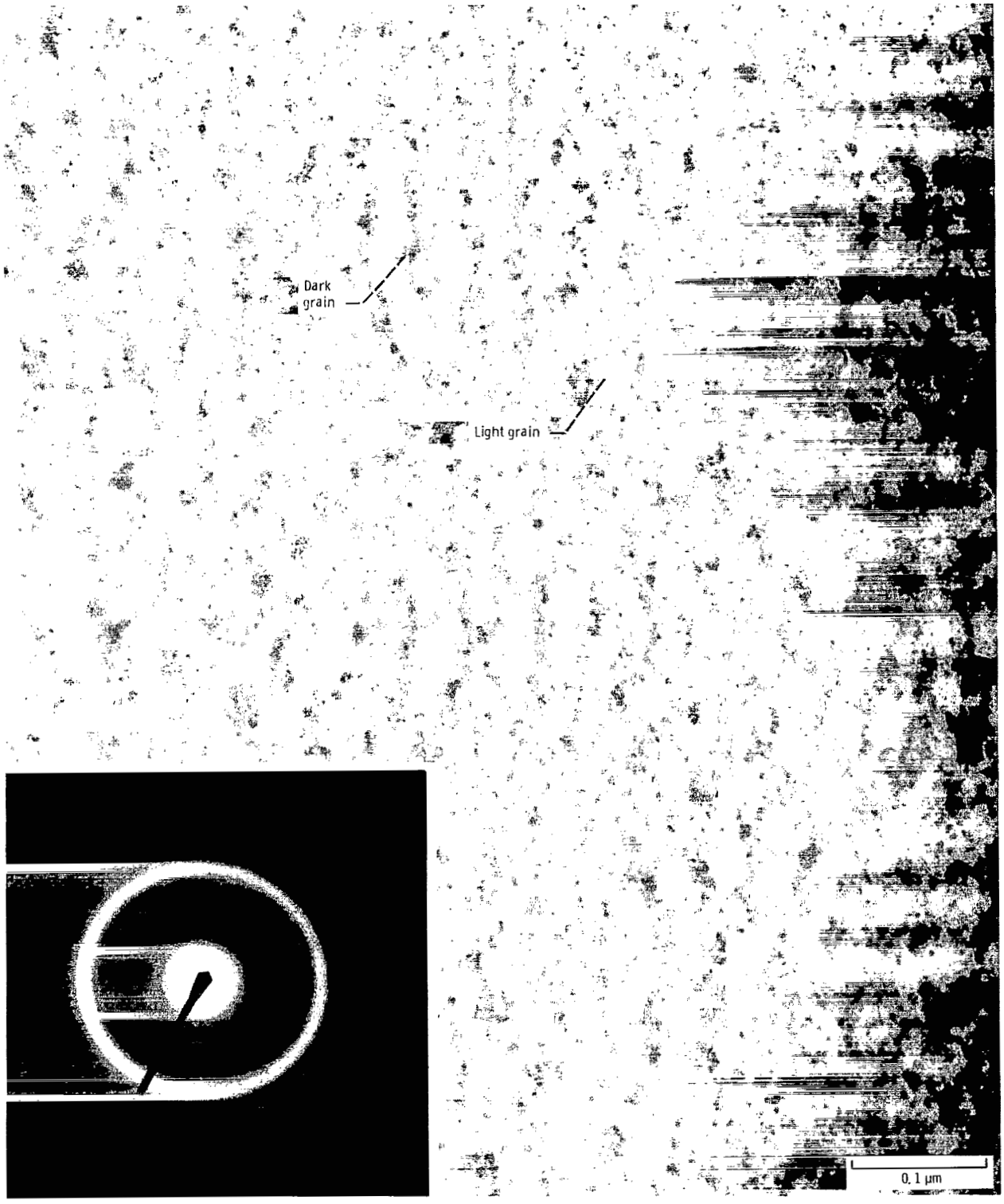

Figure 12. - Typical microstructure and electron diffraction patterns of a metallic glass ($Fe_{67}Co_{18}B_{14}Si_1$).

Figure 13. - Typical microstructure and electron diffraction patterns of wear surface of metallic glass ($Fe_{67}C_{18}B_{14}Si_1$). Rider, 3.2-millimeter-diameter aluminum oxide sphere; load, 2.5 newtons; sliding velocity, 1.5 millimeters per second; sliding time, 150 hours; sliding distance, 810 meters; room temperature; laboratory air atmosphere.

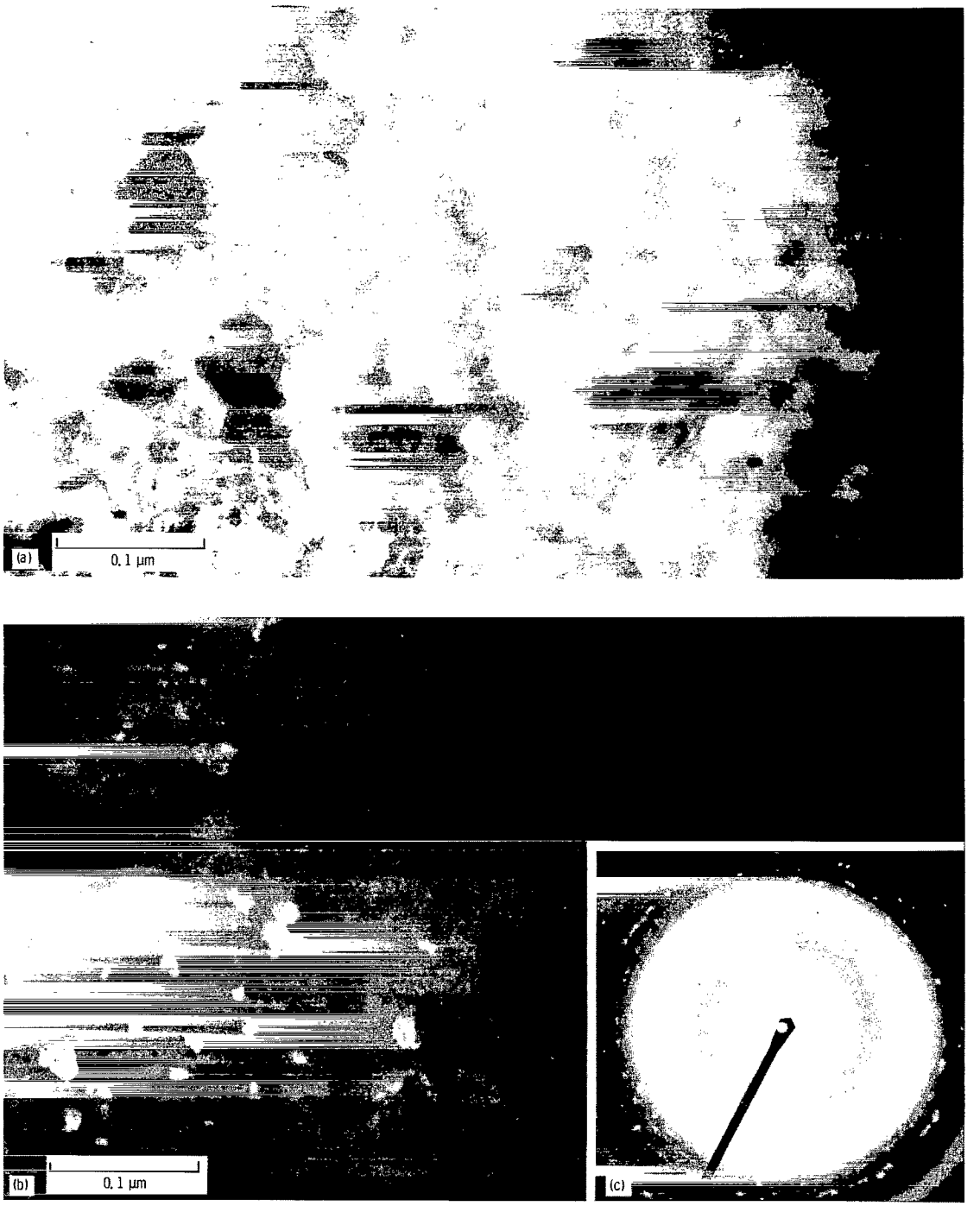

(a) Bright field.

(b) Dark field.

(c) Diffraction pattern.

Figure 14. - Microstructure and electron diffraction patterns of wear surface of metallic glass ($Fe_{67}Co_{18}B_{14}Si_1$). Rider, 3.2-millimeter-diameter aluminum oxide sphere; load, 2.5 newtons; sliding velocity, 1.5 millimeters per second; sliding time, 150 hours; sliding distance 810 meters; room temperature; laboratory air atmosphere.

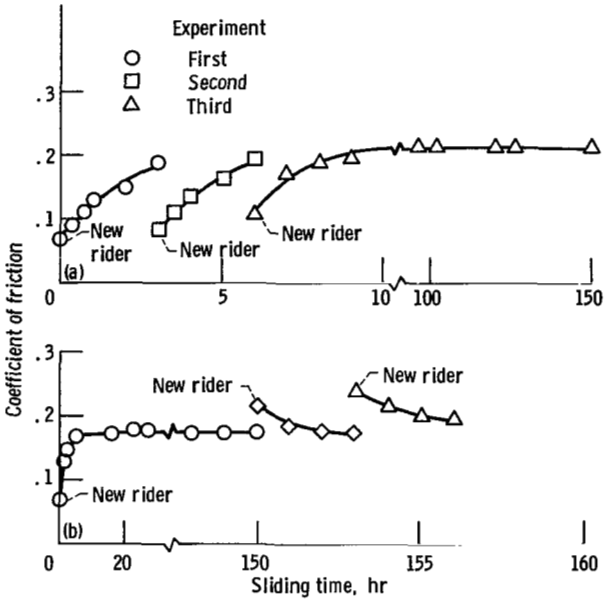

(a) Sliding time, 0 to 150 hours.
(b) Sliding time, 0 to 156 hours.

Figure 15. - Coefficient of friction as function of sliding time for $Fe_{67}Co_{18}B_{14}Si_1$ amorphous alloy in laboratory air atmosphere. Rider, 3.2-millimeter-diameter aluminum oxide sphere; load, 2.5 newtons; sliding velocity, 1.5 millimeters per second; room temperature.

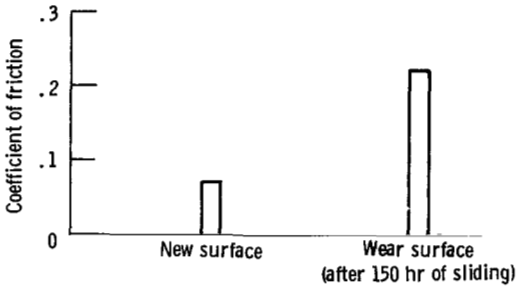

Figure 16. - Coefficients of friction for new and wear surfaces (sliding period, 150 hr) of $Fe_{67}Co_{18}B_{14}Si_1$ amorphous alloy. Rider, 3.2-millimeter-diameter aluminum oxide sphere; load, 2.5 newtons; sliding velocity, 1.5 millimeters per second; room temperature.

of friction obtained in the second experiment was due to the crystallization of the alloy described earlier. The coefficient of friction decreased with increasing sliding time in the second experiment until ultimately the same value was obtained as in the first experiment. The coefficient of friction after the 3-hour sliding period in the second experiment was the same as that obtained after 150 hours of sliding in the first experiment. After 3 hours of sliding, oxide wear debris particles were observed. Thus, the transient friction in the second experiment is due to the generation of oxide wear debris particles.

The friction and wear behavior of the amorphous alloy in the third experiment was very similar to that of the second experiment. Thus, crystallization of the wear surface of the amorphous alloy causes high friction. Generation of oxide wear debris particles on the amorphous alloy causes transitions

in friction behavior. Oxide wear debris particles may contribute to increased friction of the amorphous alloy in the amorphous state. On the other hand, they contribute to decreased friction of the wear surface of the amorphous alloy in the crystalline state.

Figure 16 presents the friction data obtained for amorphous alloys (1) with a new surface and (2) with a wear surface with 150 hours of sliding. The difference in friction between the new and wear surfaces is based on crystallographic characteristics. The coefficient of friction of the amorphous alloy increases with crystallization of the alloy. This is consistent with the authors' earlier studies (refs. 3 and 4).

CONCLUSIONS

As a result of transmission electron microscopy, diffraction studies, and sliding friction and wear experiments conducted with $Fe_{67}Co_{18}B_{14}Si_1$ ferrous-base metallic glass in contact with a 3.2-millimeter-diameter aluminum oxide rider in laboratory air atmosphere, the following conclusions are drawn:

1. An amorphous alloy can be crystallized during the sliding process. Crystallites with sizes of 10 to 150 nanometers are produced on the wear surface of the amorphous alloy. Crystallization of a wear surface of an amorphous alloy causes higher friction.
2. Plastic flow occurs on an amorphous alloy surface with sliding, and the flow film of the alloy transfers to the aluminum oxide rider surface.
3. Two distinct types of wear debris were observed as a result of sliding: an alloy wear debris, and powdery and whiskery oxide debris. Generation of oxide wear debris particles on an amorphous alloy surface causes transitions in friction behavior. Oxide wear debris particles contribute to increased friction of the alloy in the amorphous state. On the other hand, they contribute to decreased friction of the wear surface of the alloy in the crystalline state.

Lewis Research Center
National Aeronautics and Space Administration
Cleveland, Ohio, August 26, 1982

REFERENCES

1. DeCristofaro, N.; and Henschel, C.: Metglas Brazing Foil. Weld. J., vol. 5, no. 7, July 1978, pp. 33-38.
2. Amuzu, J. K. A.: Sliding Friction of Some Metallic Glasses. J. Phys., D, vol. 13, 1980, pp. L127-L129.
3. Miyoshi, K.; and Buckley, D. H.: Friction and Surface Chemistry of Some Ferrous-Base Metallic Glasses. NASA TP-1991, Mar. 1982.
4. Miyoshi, K.; and Buckley, D. H.: Surface Chemistry, Microstructure, and Friction Properties of Some Ferrous-Base Metallic Glasses at Temperatures to 750° C. NASA TP-2006, Apr. 1982.
5. Gilman, J. J.: Metallic Glasses. Phys. Today, vol. 28, no. 5, Mar. 1975, pp. 46-53.
6. Scott, V. D.; and Wilman, H.: Surface Re-orientation Caused on Metals by Abrasion - Its Nature, Origin and Relation to Friction and Wear. Proc. Roy. Soc. London, vol. A247, no. 1250, Sept. 30, 1958, pp. 353-368.

7. Goddard, J.; Harker, H. J.; and Wilman, H.: The Surface Reorientation Caused by Uni-directional Abrasion on Face-Centred Cubic Metals. Proc. Phys. Soc. London, vol. 80, no. 3, Sept. 1962, pp. 771-782.
8. Buckley, D. H.: Recrystallization and Preferred Orientation in Single-Crystal and Polycrystalline Copper in Friction Studies. NASA TN D-3794, 1967.

1. Report No.	2. Government Accession No.	3. Recipient's Catalog No.
NASA TP-2140		

4. Title and Subtitle

SLIDING INDUCED CRYSTALLIZATION OF METALLIC GLASS

5. Report Date
March 1983

6. Performing Organization Code
506-53-12B

7. Author(s)

Kazuhisa Miyoshi and Donald H. Buckley

8. Performing Organization Report No.
E-1278

10. Work Unit No.

9. Performing Organization Name and Address

National Aeronautics and Space Administration
Lewis Research Center
Cleveland, Ohio 44135

11. Contract or Grant No.

13. Type of Report and Period Covered
Technical Paper

12. Sponsoring Agency Name and Address

National Aeronautics and Space Administration
Washington, D. C. 20546

14. Sponsoring Agency Code

15. Supplementary Notes

16. Abstract

Sliding friction and wear experiments, electron microscopy, and diffraction studies were conducted with an $Fe_{67}Co_{18}B_{14}Si_1$ ferrous-base metallic glass in sliding contact with aluminum oxide at room temperature in air. The results indicate that the amorphous alloy can be crystallized during the sliding process. Crystallization of the wear surface causes high friction. Plastic flow occurred on the amorphous alloy with sliding, and the flow film of the alloy transferred to the aluminum oxide surface. Two distinct types of wear debris were observed as a result of sliding: an alloy wear debris, and powdery and whiskery oxide debris. Generation of oxide wear debris particles on an alloy can cause transitions in friction behavior.

17. Key Words (Suggested by Author(s))	18. Distribution Statement
Metallic glass Wear Crystallization	Unclassified - unlimited STAR Category 26

19. Security Classif. (of this report)	20. Security Classif. (of this page)	21. No. of Pages	22. Price*
Unclassified	Unclassified	24	A02

* For sale by the National Technical Information Service, Springfield, Virginia 22161

NASA-Langley, 1983

4 1 1U,C, 830310 S00903DS
DEPT OF THE AIR FORCE
AF WEAPONS LABORATORY
ATTN: TECHNICAL LIBRARY (SUL)
KIRTLAND AFB NM 87117